Dissociative adsorption of H on Cu(100): A four-dimensional study of the effect of rotational motion on the reaction dynamics. Erratum.

Mowrey, R.C.; Kroes, G.J.; Wiesenekker, G.; Baerends, E.J.

published in
Journal of Chemical Physics
1999

DOI (link to publisher)
10.1063/1.478794

document version
Publisher's PDF, also known as Version of record

Rotational effects in six-dimensional quantum dynamics for reaction of H_2 on Cu(100)

Drew A. McCormack[a] and Geert-Jan Kroes
Leiden Institute of Chemistry, Gorlaeus Laboratories, Leiden University, P.O. Box 9502, 2300 RA Leiden, The Netherlands

Roar A. Olsen and Evert-Jan Baerends
Theoretical Chemistry, Free University, De Boelelaan 1083, 1081 HV Amsterdam, The Netherlands

Richard C. Mowrey
Theoretical Chemistry Section, Code 6179, Naval Research Laboratory, Washington, District of Columbia 20375-5342

(Received 14 September 1998; accepted 11 January 1999)

We present results of six-dimensional (6D) quantum wave-packet calculations for the dissociative adsorption of $(\nu=0,j=4,m_j)$ H_2 on Cu(100). The potential-energy surface is a fit to points calculated using density-functional theory (DFT), with the generalized gradient approximation (GGA), and a slab representation for the surface. New aspects of the methodology we use to adapt the wave function to the symmetry of the surface, which relate to calculations for initial rotational states with odd m_j (the magnetic quantum number), are explained. Invoking detailed balance, we calculate the quadrupole alignment for H_2 as it would be measured in an associative desorption experiment. The reaction of the helicopter $(\nu=0,j=4,m_j=4)$ state is preferred over that of the $(\nu=0,j=4,m_j=0)$ cartwheel state for all but the lowest collision energies considered here. The energy dependence of the quadrupole alignment that we predict for $(\nu=0,j=4)$ H_2 desorbing from Cu(100) is in good qualitative agreement with velocity-resolved associative desorption experiments for D_2+Cu(111). The vibrational excitation probability $P(\nu=0,j\rightarrow\nu=1)$ is much larger for $j=4$ than for $j=0$, and the m_j-dependence of $P(\nu=0,j=4,m_j\rightarrow\nu=1)$ is markedly different from that of the initial-state-resolved reaction probability. For all but the highest collision energies, vibrational excitation from the $(\nu=0,j=4)$ state is accompanied by loss of rotational energy, in agreement with results of molecular beam experiments on scattering of H_2 and D_2 from Cu(111).
 [S0021-9606(99)71014-7]

I. INTRODUCTION

Developments in experimental and theoretical methods are continually shedding new light on molecule-surface scattering. Utilizing the two approaches in a complimentary fashion, the deficiencies of one can be balanced by the strengths of the other, thereby improving our overall understanding of the interactions and mechanisms involved. Such is the case for reactions of H_2 on Cu surfaces. Associative desorption experiments are at a point where simultaneous measurement of the desorbing molecules' velocity, vibrational state ν, angular momentum j, and quadrupole alignment (distribution over m_j) can be achieved.[1] From the point of view of calculations, it is now possible, although expensive, to perform fully quantum calculations for all six degrees of freedom of a diatomic molecule incident on a surface.[2–8] When taken together, these two approaches offer a powerful means with which to probe a given system. Currently, strong aim is being taken in both fields at revealing the intricacies of rotational effects in surface processes. By presenting results of quantum six-dimensional (6D) calculations for several initial rotational states of H_2 reacting on Cu(100), and interpreting them against the backdrop of experimental research, we hope to contribute to an increased understanding of rotational effects in surface scattering.

Experimentally, associative desorption experiments[1,9–11] have been most useful for studying rotational effects in reactions at surfaces. These can utilize time-of-flight techniques to measure the velocity of desorbing molecules, and spectroscopic techniques to detect the vibrational state ν and angular momentum j as well as, in some cases, the quadrupole alignment of the desorbing molecules. Using detailed balance, Rettner *et al.* derived dissociation probabilities which were resolved with respect to the velocity and rovibrational (ν,j) state of H_2 reacting with Cu(111).[12] They concluded that rotation inhibited reaction for $j<4$ and enhanced it for $j>4$, but no consideration was given to rotational orientation (i.e., alignment). Wetzig *et al.*[10] and Gulding *et al.*[11] then performed measurements, independently of one another, on D_2+Cu(111), to establish the alignment of molecules desorbing in a rovibrational (ν,j) state, averaging over the desorption energy. Wetzig *et al.* found essentially zero alignment for all $(\nu=0,j)$ states investigated $(j=2-8)$. This finding was reproduced by Gulding *et al.* for $(\nu=0,j)$ states with j ranging from 1 to 4, but they measured positive alignments which increased with j for the other $(\nu$

[a]Electronic mail: mccormac@chem.leidenuniv.nl

$=0,j$) states examined ($j=5-7$, 9, and 10). (Positive alignment indicates a preference for helicopter-type motion.) Most recently, Hou *et al.* have additionally examined the translational energy dependence of the alignment of D_2 molecules desorbing from Cu(111) in two particular (ν,j)-states.[1] For each of the rovibrational states considered, they observed a positive alignment at low translational energies which decreased with increasing energy.

None of these desorption experiments were performed for the particular system that we address here: H_2+Cu(100). While associative desorption[13] and molecular beam[14] experiments have been undertaken for H_2+Cu(100), no study of rotational effects has yet been published. The most complete analysis of the existing experiments was performed by Michelsen and Auerbach;[15] by constructing a vibrational state dependent model, they were able to reconcile data from the two separate experiments (associative desorption[13] and molecular beam[14]) to produce a single consistent set of results. Unfortunately, whilst these findings offer insight into vibrational effects, rotation was not considered in the model (nor could it be, given the available data).

This state of affairs offers a unique opportunity for theory to take the lead from experiment. It is only recently that the first quantum calculations to treat all six dimensions of H_2 reacting on Cu(100) have become viable.[2] Such calculations have now been performed for various initial states,[3,4] and similar calculations have been carried out on H_2+Cu(111).[5,6] Previous to these, theoretical studies of surface reactions were restricted to explaining experimental trends, because to obtain a quantitatively accurate picture of dissociative chemisorption of diatomic molecules on metal surfaces, it is necessary to consider all six molecular degrees of freedom.[2,16–18] Nonetheless, reduced dimensionality (2D–4D) calculations[16,19–27] have played, and will continue to play, a very important role in understanding the trends found experimentally.

Low-dimensionality calculations have provided much of the detail that makes up our current understanding of rotation in surface reactions. Two-dimensional model calculations were performed by Brunner and Brenig on D_2+Cu(111).[27] In other studies of the Cu(111) surface, Darling and Holloway were able to reproduce the trend seen experimentally that rotation inhibits reaction for low j, and enhances it at high j.[16,28] More importantly, they were able to verify the explanation offered by Michelsen *et al.*[29] that the phenomenon was due to a balance between steric effects, and coupling between the rotational modes and the reaction coordinate.[28] These and other reduced-dimension calculations[23,30,31] for the Cu(111) surface also predicted preferred reaction of helicopter states ($|m_j|=j$). Invoking microreversibility, the results of the reduced dimensionality calculations on H_2[16,23] have been compared to the experimental, desorption energy averaged alignment of D_2 desorbing from Cu(111).[9,11] The outcome of these comparisons[9,11] suggested that the calculations significantly overestimated the preference for helicopter reaction.

Just recently, Dai and Light have performed 6D wave-packet calculations for dissociation of H_2 on Cu(111) for a range of initial (ν,j,m_j) states.[5] The potential-energy surface (PES) used[23] was a London–Eyring–Polanyi–Sato (LEPS) potential fitted to points calculated by DFT with the generalized gradient approximation (GGA).[32] Their results enabled them to arrive at a direct comparison with the velocity resolved, associative desorption experiments of Hou *et al.* for $(\nu=0,j=11)$ and $(\nu=1,j=6)$ D_2 desorbing from Cu(111).[1] Theory and experiment are in good agreement for the alignment of the desorbing molecules as a function of $E-E_0(\nu,j)$, where E is the desorption or collision energy, and $E_0(\nu,j)$ is the kinetic barrier height [the collision energy at which the dissociation probability of (ν,j) H_2 (or D_2) becomes half its saturation value]. The theory thus reproduces the experimental finding of positive alignment in desorption, the alignment decreasing with increasing desorption energy, for the two cases studied. One reason that the energy shift [by $E_0(\nu,j)$] was necessary is that the experiments were performed for D_2 and the calculations for H_2, the $E_0(\nu,j)$ values being quite different for the two different isotopes, for both (ν,j) states studied. The positive outcome of the comparison suggests that combining the use of a 6D quantum dynamical method with that of a PES taken from density functional theory (DFT) constitutes a successful approach to the calculation of alignment in associative desorption.

Thus far, we have obtained results of 6D quantum calculations on H_2+Cu(100) for initial states with $j=0$,[2,3] and ($j=4$, $m_j=0$ and 4).[4] As far as rotational effects are concerned, only the $j=4$ results are of interest. We found that, in agreement with theoretical and some of the experimental findings for $H_2(D_2)$+Cu(111), helicopter reaction was preferred over cartwheel reaction, for the greater part of the range of collision energies considered. However, without results for all the states in the $j=4$ manifold, no predictions could be made about the overall reaction probability for $j=4$, or the orientational distribution of the angular momentum vector (e.g., the quadrupole alignment) that would be seen in desorption, which are the quantities most useful for comparison with experiments that can currently be performed.

In this paper we address this by presenting data for all $j=4$ rotational states, and further derive the translational energy dependence of the $j=4$ reaction probability and the alignment, as would be measured in associative desorption experiments. For desorption energies larger than $E_0(\nu=0,j=4)-0.2$ eV, our predictions for H_2+Cu(100) are in agreement with previous experiments and 6D quantum-mechanical calculations on $H_2(D_2)$+Cu(111), in that the alignment is a positive, decreasing function of the desorption energy. The present calculations for H_2+Cu(100) also predict that the reaction of $(\nu=0,j=4)$ H_2 is weakly preferred over that of $(\nu=0,j=0)$ H_2 at most collision energies, which is at odds with previous experimental and theoretical results for H_2+Cu(111). However, as will be explained below, this preference is possibly a result of limitations in the potential model used. Interesting findings, which are relevant to previous experiments[33] on vibrational excitation of H_2 scattering from Cu(111), are that the vibrational excitation probability $P(\nu=0,j\rightarrow\nu=1)$ is much larger for $j=4$ than for $j=0$, and that the m_j-dependence of the vibrational excitation prob-

ability $P(\nu=0,j=4,m_j \rightarrow \nu=1)$ is different from that of the reaction probability $R(\nu=0,j=4,m_j)$.

In Sec. II, we describe the methods that are used in the electronic structure and dynamics calculations. In particular, Sec. II A 1 gives a description of the improved PES that we have used in the present and previous[4] 6D calculations on the reaction of rotationally excited H_2. Compared to the PES[34] used in earlier calculations for the reaction of $(\nu=0,j=0)$ and $(\nu=1,j=0)$ H_2,[2,3] the PES used here has been improved by removing an artificial well that was present in the entrance channel and affected our earlier 6D results for these rovibrational states. In addition, we assess how the limitations of the present PES affect the reliability of our results for alignment. For that, we also compute the azimuthal dependence of the potential at an asymmetric transition state geometry which is not incorporated in the current PES fit, but which has been shown by earlier DFT calculations[35,36] to exhibit a barrier to reaction even lower than the minimum barrier in our PES. The method used in these additional electronic structure calculations is described in Sec. II A 2. Most of the methodology used in the wave-packet calculations has been documented elsewhere and is thus only briefly covered here. In Sec. II B we nevertheless present considerable detail about the symmetry-adapted basis set for the scattering wave function, because the construction of a basis set for odd-m_j initial states differs somewhat from the cases treated previously.

In Sec. III A we present the results of the electronic structure calculations for the azimuthal dependence of the potential at the asymmetric transition state barrier mentioned above. Results are also presented for the symmetric bridge-to-hollow barrier geometry, to assess how well these results compare to results of calculations which use a different implementation of the DFT/GGA/slab method, and to assess the dependence of the results on the particular GGA used. While the latter results are not as directly related to the main subject of the paper, they are interesting in their own right. Section III B presents the results of the dynamics calculations, and Sec. IV concludes.

II. METHOD

A. Electronic structure

1. PES used in dynamics

The potential used in the dynamics calculations is a fit to points which were calculated using the DFT/GGA/slab method.[34] Before we comment on the aspects of the PES that are particularly relevant to the dynamics calculations presented in this paper, we first note that in the present work, like in our previous calculations for $(\nu=0,j=4,m_j)$ H_2,[4] we use an improved version of the PES[34] used in our first 6D calculations.[2,3] The first PES contained an artificial well (of depth 0.19 eV) for the bridge-to-top dissociation geometry with $\theta=90°$ at $Z=7a_0$ and $r=1.4a_0$, which arose because the three-body term V_{3b}^A [Eq. (6a) of Ref. 34] did not extrapolate to zero fast enough at large Z for this dissociation geometry. In the new PES, this problem has been removed by multiplying the V_{3b}^A term for this dissociation geometry with a damping function [Eq. (2) of Ref. 34 which turns off V_{3b}^A between 5.0 and $5.8a_0$].

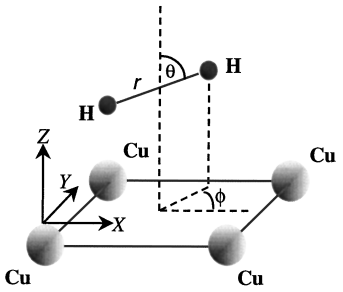

FIG. 1. The coordinate system used in calculations. The origin is at a top site.

The PES is expanded in seven symmetry-adapted functions of X, Y, θ, and ϕ (see Fig. 1), such that the PES describes the dependence of the molecule–surface interaction on θ and ϕ up to second order in spherical harmonics above the high-symmetry top, bridge, and hollow sites. For impacts of the molecule on the low-symmetry intermediate sites, the 6D potential is effectively obtained by interpolating the potentials computed for the high-symmetry sites. These limitations were imposed to make the construction of the PES computationally feasible, while at the same time modeling those aspects which were thought to be essential for obtaining a reasonable description of the reaction of H_2 in (ν,j) states with j not too high. Thus, the present PES should give a reasonable description of the polar and azimuthal dependence of the potential at the high-symmetry site with the lowest associated symmetry (i.e., the twofold bridge site). It was assumed that correctly describing the azimuthal dependence of the higher symmetry (fourfold top and hollow) sites should be somewhat less important, and the potential was thus taken azimuthally flat at these sites. The present PES should provide a reasonable description of the potential's dependence on θ at these sites, but its independence on ϕ is an approximation, which could be particularly severe for the hollow site (dissociation of the atoms to the bridge and top sites being exothermic and endothermic, respectively). The fact that the potential is taken as azimuthally flat over these sites may well lead to computed alignment values which are too high, especially at higher collision energies [the barriers to dissociation over the top and hollow sites (0.70 and 0.64 eV) are larger than the minimum barrier to dissociation obtained for the bridge site (0.48 eV)].

Because for low-symmetry sites the potential is found by extrapolation, for these sites the size of the azimuthal anisotropy of the PES is intermediate between that of the bridge and the other two high-symmetry sites in the model. To see whether this would be realistic, calculations were also performed for a dissociation geometry which is intermediate between the bridge-to-hollow and hollow-to-bridge geometries which are incorporated in the PES. [Other electronic structure calculations[35,36] had suggested that the minimum barrier to dissociation associated with this intermediate geometry should be slightly lower than for the symmetric bridge-to-hollow geometry (by about 30 meV), provided the

TABLE I. The basis sets used in the slab calculations. An NAO is a numerical atomic orbital obtained from a Herman–Skillman type calculation (Ref. 41). An STO is a Slater-type orbital with the given exponent. For Cu a frozen core approximation has been used up to and including $3p$.

	Cu				H		
	$3d$	$4s$	$4p$	$4f$	$1s$	$2p$	$3d$
NAO	yes	yes	no	no	yes	no	no
STO	1.28, 6.90	0.85, 2.45	1.0, 2.0	1.5	0.69, 1.58	1.25	2.5

molecule tilts out of the surface plane.] These calculations are described in Secs. II A 2 and III A. The results show that for this site the present PES also underestimates the azimuthal anisotropy. Combined with our previous discussion of the PES for H_2 approaching the top or hollow site, this finding means that calculations with the present PES will probably overestimate the alignment in desorption for all desorption energies.

2. New electronic structure calculations

We have used the ADF-BAND program[37,38] to perform density functional theory (DFT) calculations employing the local density approximation (LDA) and two different generalized gradient approximations (GGAs) for a selected set of geometries. The ADF-BAND program solves the Kohn–Sham equations[39,40] self-consistently for a periodic system—in our case a semi-infinite slab with translational symmetry in two directions. A flexible basis set consisting of a combination of numerical atomic orbitals (NAOs) obtained from numerical Herman–Skillman-type calculations[41] and Slater-type orbitals (STOs) is used in the expansion of the one-electron states. The frozen core approximation can be used for the core electrons of the heavier atoms, thus avoiding the use of pseudopotentials. In calculating the matrix elements of the Hamiltonian the program employs an accurate Gauss-type numerical integration scheme,[38] and the **k**-space integration is performed by the quadratic tetrahedron method.[42] No shape approximations are made to the potentials.

The Vosko–Wilk–Nusair formulas[43] are used for the exchange-correlation energy in the LDA. For the GGAs we use the Becke correction[44] for the exchange energy and the Perdew correction[45] for the correlation energy (BP). The other GGA we give results for in this study is the gradient-corrected functional of Perdew *et al.*[46,47] (PW GGA-II, which we will label PW for brevity). The gradient corrections are calculated from the self-consistent LDA density, which has been shown to be an excellent approximation to the binding energies calculated from the self-consistent nonlocal densities.[32] The present calculations include a thicker slab, larger basis set, and more accurate integration than those used previously to calculate the 6D PES.[34]

Hydrogen is adsorbed on one site of a three layer Cu(100) slab within a 2×2 surface unit cell. The basis set we use is given in Table I and it should give results very close to the basis set limit. The **k**-space integration is done with 25 points in the irreducible wedge of the surface Brillouin zone (SBZ), corresponding to a total of 41 points in the whole SBZ. For the real-space integration the ''accint'' parameter[48] is set to 4.5. With these parameter choices our results are converged to within 0.05 eV of the three layer DFT results for the different functionals. Calculations with a smaller basis set show that changing the number of layers from 3 to 5 only results in a small change (by $+0.02$ eV) in interaction energy.

B. Wave-packet method

The Hamiltonian used to describe the motion of the H_2 molecules, in terms of the coordinates shown in Fig. 1, is given by

$$\hat{H}=-\frac{1}{2M}\left(\frac{\partial^2}{\partial Z^2}+\frac{\partial^2}{\partial X^2}+\frac{\partial^2}{\partial Y^2}\right)-\frac{1}{2\mu}\frac{\partial^2}{\partial r^2}+\hat{H}_{\rm rot}+V(Z,X,Y,r,\theta,\phi), \tag{1}$$

where M is the mass of H_2; μ, its reduced mass; and $\hat{H}_{\rm rot}$, the rotational Hamiltonian of the molecule. In deriving Eq. (1) we have adopted the usual approach of multiplying the wave function by r, and redefining the inner product on r appropriately.[49] The potential energy, V, is the PES that has been described in Sec. II A 1.

In this and previous studies,[2–4] we treat only reaction at normal incidence. This is reasonable because experimental results indicate that the H_2+Cu(100) reaction obeys normal energy scaling (i.e., the reaction probability is dependent only on the component of translational energy perpendicular to the surface).[15] Not considering off-normal incidence allows for a dramatic reduction in computation cost (the calculations, as currently performed, would probably be infeasible otherwise). This saving is made by reducing the scale of the basis used to represent the wave function through adaptation to the surface symmetry (C_{4v}).[50,51]

The wave function, $\Psi^{\nu_0 j_0 m_{j0}}(t)$, is represented in a close-coupling wave-packet fashion using a grid in Z and r, and basis functions in X, Y, θ, and ϕ, such that

$$\Psi^{\nu_0 j_0 m_{j_0}}(t)=\sum_{\Gamma^\alpha j m_j \Gamma_d^\alpha n m} f^{\nu_0 j_0 m_{j_0}}_{\Gamma^\alpha j m_j \Gamma_d^\alpha n m}(Z,r;t)\times g_{\Gamma^\alpha j m_j \Gamma_d^\alpha n m}(X,Y,\theta,\phi). \tag{2}$$

The quantum numbers of the initial state are subscripted by a ''0.'' The standard labeling of states applies: ν is for the vibrational state, and j and m_j for the rotation. Because the potential is periodic with respect to X and Y, parallel motion is quantized with diffraction quantum numbers given by n and m. The overall symmetry of rotation–diffraction function g is given by Γ^α, the αth partner of symmetry species Γ in the C_{4v} point group. The symmetry of the diffraction function in g is given by Γ_d^α.

The theory for setting up the symmetry-adapted (SA) bases has been given elsewhere, for $m_j=0$ initial states,[51] and m_j-even states.[4] In short, for m_j zero only SA functions of the totally symmetric A_1 species need be included in the wave-packet calculation, and with m_j even, two separate wave-packet calculations are required, one for each symmetry species contributing to the nonsymmetry-adapted (NSA)

initial state. Because we also perform calculations here for m_j-odd initial states, details of how these are treated will be given here.

The difficulty in constructing a suitable basis for m_j-odd states is that the NSA initial state cannot be decomposed into a superposition of SA functions from one-dimensional irreducible representations (or irrep's). In particular, these NSA initial states can only be represented as a superposition of two E-type functions.[52,53]

The direct product relations of the C_{4v} group that are of relevance here are[52,53]

$$\Gamma \otimes E = E \quad \text{for} \quad \Gamma = A_1,\ A_2,\ B_1,\ \text{and}\ B_2. \tag{3}$$

We can form a rotation–diffraction basis of E-type functions by taking the diffraction and rotation functions given in Ref. 48 and combining them according to the following identities:[54]

$$\begin{aligned} g_{E^1} &= a_1.e^1, \quad g_{E^2} = a_1.e^2, \\ g_{E^1} &= a_2.e^2, \quad g_{E^2} = -a_2.e^1, \\ g_{E^1} &= b_1.e^1, \quad g_{E^2} = -b_1.e^2, \\ g_{E^1} &= b_2.e^2, \quad g_{E^2} = b_2.e^1, \end{aligned} \tag{4}$$

where E^1 and E^2 designate ''partners'' in the E irrep,[52] g_{E^1} and g_{E^2} are the rotation–diffraction basis functions, and the lower-case letters denote rotation and diffraction functions of the indicated symmetry (e.g., a_1 is a function of symmetry A_1). In Eq. (4), signs have been included to ensure that partner rotation–diffraction functions belong to the same E irrep (see below). Next, one uses that[55]

$$\langle g_{\Gamma^\alpha \kappa} | \hat{V} | g_{\Gamma'^{\alpha'} \kappa'} \rangle = 0 \quad \text{if} \quad \Gamma'^{\alpha'} \neq \Gamma^\alpha, \tag{5}$$

where κ is used in place of all excluded subscripts (i.e., j, m_j, n, m, and Γ_d^α). This expression indicates not only that the potential cannot couple states of different symmetry species, but also that it is incapable of coupling states of the same species that belong to different partner representations (in the case of normal incidence, the kinetic-energy operator is also unable to couple these states). In the present calculations this means that an initial rotation–diffraction state with symmetry E^1 cannot populate a state with symmetry E^2, and *vice versa*.

Next we use that[55]

$$\langle g_{\Gamma^\alpha \kappa} | \hat{H} | g_{\Gamma^\alpha \kappa'} \rangle = \langle g_{\Gamma^{\alpha''} \kappa} | \hat{H} | g_{\Gamma^{\alpha''} \kappa'} \rangle. \tag{6}$$

That is, the coupling induced between two states of the same species and partner type, will be exactly the same as that induced between their corresponding partner states. As a result, the S-matrix evaluated in the basis of one partner symmetry is the same as that of the other partner symmetry. This means that to obtain results for the odd m_j states, one only has to perform a calculation for one partner symmetry.

Some clarification should be made at this point as to how the rotation–diffraction symmetry-adapted functions should be formed. In many instances it is possible to take liberties with regard to multiplicative constants and signs in deriving a basis set. For example, the basis function $\sin\theta$ is just as good for most purposes as $-i\sin\theta$. Here, however, care must be taken to ensure that the rotation–diffraction functions in one basis (e.g., E^1) are true partners to the functions in the other basis (e.g., E^2). A sign change in one of the functions, or multiplication by a constant, will mean that Eq. (6) will not hold, and the extraction of results for one partner species from those of the other will be flawed. To arrive at the correct correspondence, one can use the group projection operator.[51]

One further reduction in basis size is possible in this case, due to the particular form of the PES used:[34] It is constructed entirely from rotation and diffraction functions of A_1 and B_1 symmetry. Referring back to Eq. (4), it should become clear that this allows for a further reduction to around $\frac{1}{4}$ of the computational effort, since an A_1 diffraction function (such as the initial state) can only populate diffraction states of A_1 or B_1 symmetry.[4] Any rotation–diffraction functions which do not include an A_1 or B_1 diffraction function can be excluded from the calculation.

Having formed the symmetry-adapted basis sets—with the correct correspondence between partners—the calculations proceed almost as for even m_j states ($m_j \neq 0$), except that only one wave-packet calculation is performed, for one of the two partner species. Results for both species can be derived from this single calculation. The overall saving in computational expense is on a par with that for m_j-even states.[4] The reason that these calculations are not more efficient, given that only one wave-packet calculation is required instead of the two needed for m_j-even, is that the basis size is around twice as large.

We use the absorbing boundary condition (ABC) evolution operator to propagate the wave packet,[3,56] and adopt a real initial wave function of the form[3]

$$\Psi^{\Gamma^\alpha \nu_0 j_0 m_{j_0}} = \varphi_{\nu_0 j_0}(r) g_{\Gamma^\alpha j_0 m_{j_0} A_1 00}(X, Y, \theta, \phi) \times \int_{-\infty}^{\infty} dk'\, b(k') \frac{\exp(ik'Z)}{\sqrt{2\pi}}, \tag{7}$$

where

$$b(k) = \left(\frac{2\zeta^2}{\pi}\right)^{1/4} \{\exp[-(k_{\mathrm{av}} - k)^2 \zeta^2 + i(k_{\mathrm{av}} - k) Z_0] + \exp[-(k_{\mathrm{av}} + k)^2 \zeta^2 - i(k_{\mathrm{av}} + k) Z_0]\}, \tag{8}$$

to enable the use of real operator algebra in the expensive part of the calculation. Here $\varphi_{\nu_0 j_0}(r)$ is the initial vibrational eigenfunction; ζ, a width parameter; k_{av}, the magnitude of the average momentum associated with each Gaussian component; and Z_0, the location of the peak in coordinate Z. The ABC operator incorporates an optical potential, which absorbs the wave packet at the edge of the grid.[3,56]

The probability of scattering back into a particular gas-phase asymptotic state is calculated according to

$$P_{\nu_0 j_0 m_{j_0} \to \nu' j' m'_j n' m'}(E) = |S_{\nu_0 j_0 m_{j_0} \to \nu' j' m'_j n' m'}(E)|^2, \tag{9}$$

where the $S_{\nu_0 j_0 m_{j_0} \to \nu' j' m'_j n' m'}$ are elements of the scattering matrix, S. The initial state selective reaction probability is then simply calculated as the probability of *not* scattering into one of the gas-phase states.

Propagating a wave packet for one of the E partner symmetries yields elements of a SA S-matrix, S^{SA}. These elements, which are calculated during the propagation using the scattering amplitude formalism,[57,58] are equal to the corresponding elements of the SA S-matrix for the other partner. That is,

$$S_{E^1\nu_0 j_0 m_{j_0}\rightarrow E^1\nu' j' m'_j \Gamma'^{\alpha'}_d n' m'} = S_{E^2\nu_0 j_0 m_{j_0}\rightarrow E^2\nu' j' m'_j \Gamma'^{\alpha''}_d n' m'}, \tag{10}$$

where $\Gamma'^{\alpha'}_d$ and $\Gamma'^{\alpha''}_d$ are used here to label the symmetries of the final diffraction states, which may or may not be the same for the partners. The transformation from S^{SA} to S is given by

$$S = TS^{\mathrm{SA}}T^{\dagger}, \tag{11}$$

where T is the transformation matrix from the NSA basis, $\{\eta_\epsilon\}$, to the SA basis, $\{g_\kappa\}$, such that

$$g_\kappa = \sum_\epsilon \eta_\epsilon T_{\epsilon\kappa}. \tag{12}$$

Elements of T must be known for states of both partner species in order to calculate S.

We perform calculations here for the states ($\nu=0, j=4, m_j$). Numerical details of the calculations are relatively unchanged from previous studies.[3,4] Separate calculations are carried out for low- and high-translational energies, in order to reduce overall computational expense by utilizing a smaller basis for low energies, and a shorter propagation time for high energies. High-energy calculations are typically propagated for 20 000–30 000 a.u., and low-energy calculations for 60 000–80 000 a.u. For low-energy calculations the wave function basis includes rotation–diffraction functions with $j \leqslant 24$ and $|n|+|m| \leqslant 11$, while the high-energy calculations incorporate functions with $j \leqslant 28$ and $|n|+|m| \leqslant 14$.

III. RESULTS AND DISCUSSION

A. Electronic structure calculations

In this Section we address the following questions:

(i) How well do molecule–surface interaction energies that are computed using different implementations of the DFT/GGA/slab method agree?

(ii) Does the asymmetric transition state already mentioned in Sec. I have a lower minimum barrier than the symmetric bridge-to-hollow transition state?

(iii) How large is the azimuthal anisotropy associated with the potential at the asymmetric transition state barrier geometry?

The latter issue is especially relevant to the dynamics results presented in this paper (i.e., to the calculation of alignment).

In Ref. 59 the height of the barrier to dissociation for bridge-to-hollow reaction was found to be 0.47 eV at the BP level. In Ref. 35 the same barrier was calculated to be 0.6 eV at the PW level. Here, we have performed calculations using the transition state geometry given in Ref. 35. For this geometry, we find a barrier of 0.59 eV with the BP functional and 0.47 eV with the PW functional. The reason for the difference of 0.12 eV at the BP level between our present calculations and those in Ref. 59 is twofold. Firstly, in the present calculations we use a larger basis set, one more layer, and higher integration accuracy in both real space and **k**-space. Secondly, our calculations are performed with a slightly different geometry; in Ref. 59 the transition state is located at $r=2.3\,a_0$ and $Z=2.0\,a_0$, whereas here we have used the geometry given in Ref. 60, $r=2.54\,a_0$ and $Z=1.98\,a_0$. The difference of 0.13 eV at the PW level between our results and those of Kratzer and co-workers[35] can probably be explained by (i) our calculations being better converged with respect to the **k**-space integration; (ii) our use of the frozen core approximation *versus* their use of pseudopotentials; (iii) our basis set giving results which are probably closer to the basis set limit; and (iv) their results being better converged with respect to the number of layers used in the calculations.

In Ref. 35 a transition state was found with a barrier of 0.57 eV at the PW level, which is slightly lower than even that for bridge-to-hollow reaction (0.6 eV at the PW level). Using the same geometry ($X=0.96\,a_0$, $Y=2.41\,1a_0$, $Z=1.82\,a_0$, $r=2.52\,a_0$, $\theta=114°$, $\phi=0°$; see Fig. 1 for the coordinate system used) we find a barrier of 0.57 eV at the BP level and 0.44 eV at the PW level. We, therefore, reproduce the finding of Kratzer *et al.* of a lower barrier height (by ~30 meV) at the asymmetric transition state, at both levels of theory (note that the discrepancy of 0.13 eV between our PW result and that of Kratzer *et al.*[35] can be explained as above).

As was found for the symmetric bridge-to-hollow barrier geometry, there is a difference of ~0.13 eV between the interaction energies calculated with the two GGAs. This suggests that when using DFT at the GGA level care should be taken in trusting the absolute values to better than 0.1 eV and that research should also be aimed at establishing which GGA generally gives better molecule–surface interaction energies.

Since we are also interested in how the potential varies with the azimuthal angle at the asymmetric barrier geometry, we have kept all the other coordinates fixed and calculated the potential for $\phi=45°$, 90°, 135°, and 180°, giving values of 0.99, 3.55, 3.33, and 1.26 eV, respectively, at the BP level (the PW values are 0.10–0.13 eV lower). In Fig. 2 the ϕ-dependence of the potential at the asymmetric transition state geometry (with $\theta=114°$) is compared to the ϕ-dependence of the H_2+Cu(100) PES[34] at the symmetric bridge-to-hollow barrier geometry (with $\theta=90°$). At the asymmetric barrier geometry, the potential exhibits an even stronger ϕ-anisotropy than at the C_{2v} barrier geometry that is incorporated in the H_2+Cu(100) PES used below in our dynamics calculations. [Note that we refer here to the bridge site barrier as exhibiting C_{2v} symmetry because the H_2–Cu interaction potential is invariant under the symmetry operations of the C_{2v} point group at this site.] Due to the interpolation procedure we use to obtain the potential at the asymmetric barrier geometry in the present PES, the azimuthal anisotropy of the potential will be roughly half that found for the bridge-to-hollow barrier geometry. This means that the present PES underestimates the azimuthal anisotropy of the asymmetric transition state by more than 50% (see Fig. 2),

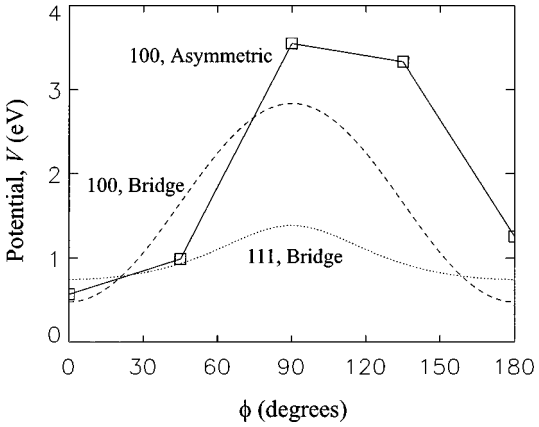

FIG. 2. Azimuthal dependence of the potential energy surface for (a) the fit used in the current calculations, (Ref. 34) with H_2 at the Cu(100) bridge site transition state; (b) the fit used in calculations for Cu(111),[6] with H_2 at the bridge site transition state; and (c) as calculated by DFT/GGA at the asymmetric minimum energy barrier for H_2+Cu(100) described in the text.

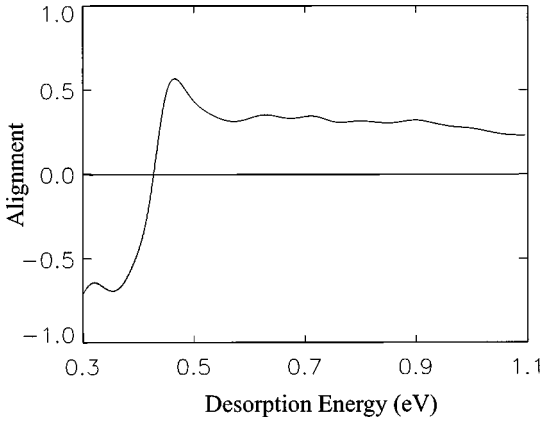

FIG. 4. The calculated quadrupole alignment vs desorption energy (eV) for ($\nu=0$, $j=4$).

and that the dynamics calculation should, therefore, overestimate the alignment of desorbing H_2 even at low desorption energies (see also Sec. II A 1).

B. Dynamics calculations

Figure 3 shows plots of the initial-state-resolved reaction probabilities $R(\nu=0,j=4,m_j)$ as a function of the collision energy E. The reaction probability for the helicopter $m_j=4$ state exceeds that of the cartwheel $m_j=0$ state for $E>0.44$ eV (see inset). At large collision energies, the reaction probability simply increases with m_j. As discussed below,

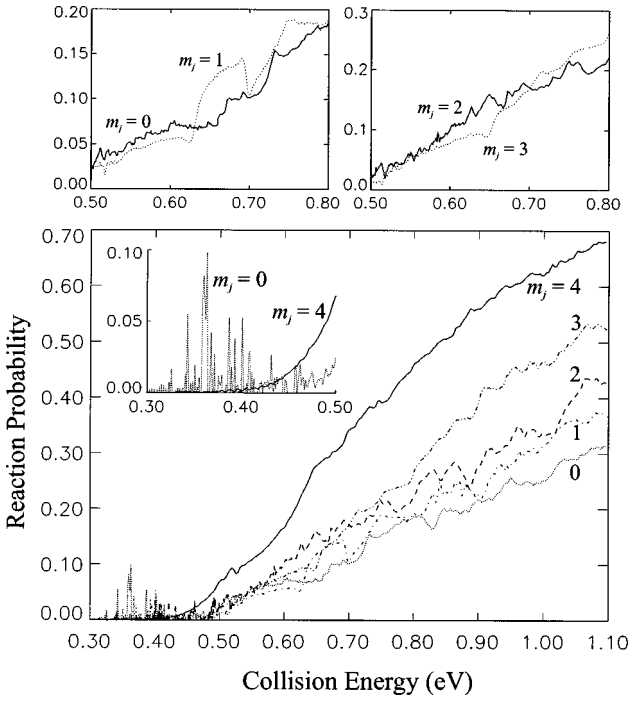

FIG. 3. Calculated reaction probabilities are shown as a function of collision energy (eV) for all ($\nu=0$, $j=4,m_j$) initial states. The inset shows the reaction probability for the $m_j=0$ and $m_j=4$ states at low collision energy. The upper plots compare reaction probabilities over an intermediate energy range for even- (excluding $m_j=4$) and odd-m_j states.

the dependence on m_j is less simple at lower energies. We first turn to a discussion of the alignment that can be computed from these results.

In Fig. 4 we have combined the results presented in Fig. 3 to calculate the quadrupole alignment that would be measured in an associative desorption experiment. This involves invoking detailed balance and thereby calculating the unnormalized associative desorption probabilities[15]

$$P_{\mathrm{des}}(E;j,m_j)=Ee^{-E/kT_s}P_{\mathrm{ads}}(E;j,m_j), \tag{13}$$

for surface temperature T_s, and desorption (collision) energy E (normal to surface). P_{ads} is the sticking probability that we get from our wave-packet calculations. The value of T_s used here is 925 K, the same as in velocity resolved experiments for D_2+Cu(111).[1] These probabilities have been convoluted with a Gaussian of full width at half maximum (FWHM) 50 meV to account for the estimated error in the measurement of desorption energy in the experiments,[61] thereby giving

$$P'_{\mathrm{des}}(E;j,m_j)=\int e^{-\alpha(E'-E)^2}P_{\mathrm{des}}(E';j,m_j)dE', \tag{14}$$

with $\alpha=1109.04\,\mathrm{eV}^{-2}$. The quadrupole alignment[62] is then given by

$$A_j^{(2)}(E)=\frac{\Sigma_{m_j}P'_{\mathrm{des}}(E;j,m_j)[3m_j^2-j(j+1)]/j(j+1)}{\Sigma_{m_j}P'_{\mathrm{des}}(E;j,m_j)}. \tag{15}$$

Figure 4 shows that the computed alignment is a positive, decreasing function of E for energies in excess of $[E_0(\nu=0,j=4)-0.2]$ eV. (We take $E_0(\nu=0,j=4)=0.69$ eV, see below. E_0 is defined as the collision energy at which the reaction probability becomes half its saturation value.) This result is in agreement with the energy dependence found in experiments which measured the alignment of D_2 desorbing in the ($\nu=0$, $j=11$) and ($\nu=1$, $j=6$) states, from Cu(111),[1] for desorption energies upwards of $[E_0(\nu,j)-0.2]$ eV. For lower desorption energies, the energy dependence of the computed alignment changes, and at low E the alignment is negative. We cannot assess whether or not this is in agreement with experiment, because experimental results were not obtained for desorption energies lower than $[E_0(\nu,j)$

$-0.2]$ eV for the two states investigated. The negative alignment we see at very low E is due to a preference for cartwheel reaction over helicopter reaction (see inset Fig. 3), where the cartwheel reaction is enhanced due to resonances which are discussed below.

Interestingly, the changed behavior of the alignment at low E (where it decreases with decreasing desorption energy) was also seen in 6D quantum dynamics calculations on H_2+Cu(111) for $(\nu=0,j)$ states with low j (see Fig. 4 of Ref. 5). This suggests that it would be of interest to extend the experiments to lower desorption energies. The explanation of the high E behavior of the alignment[1] has been that, at the lowest energies for which measurements were performed, only those molecules can react which have a favorable orientation (i.e., with their molecular axis parallel to the surface, in helicoptering states). At higher energies, more energy is available to cross the barrier, and the molecular orientation becomes less important, so that molecules in cartwheel states can also react, explaining the decreased alignment. On the basis of their results, the experimentalists ruled out an important role for steering. Steering would lead to low values of the alignment at low E, which were not observed. Our present results [and those for H_2+Cu(111)[5]] suggest that steering (by which m_j changes as the molecule approaches the barrier) could become important at low energies, but to see this experiments would have to look at lower energies than done so far.

The $A_4^{(2)}$ computed here for H_2+Cu(100) can be compared to the alignment calculated for the $(\nu=0,\ j=4)$ state of H_2 desorbing from Cu(111) by Dai and Light,[5] as long as we keep in mind the limitations of our potential model, a consideration of which suggests that our calculations should overestimate the alignment for all desorption energies (see Sec. II A 1). The $A_4^{(2)}$ computed for H_2 desorbing from Cu(111) peaks at 1.25, while our value for Cu(100) peaks at 0.57. If anything, our calculated number is too large rather than too low. This suggest that, at least at low E where the alignment is seen to peak, the alignment for H_2 desorbing from Cu(100) should be lower than for desorption from Cu(111). This is consistent with the azimuthal anisotropy of the potential at the minimum barrier geometry being much larger in the H_2+Cu(100) PES[34] than in the PES used in the dynamics calculations on H_2+Cu(111).[6] This greater anisotropy results from the molecule being closer to the surface and at greater H–H separation at the barrier geometry for the more open (100) surface [$Z=1.99a_0$ and $r=2.33a_0$ for Cu(100),[34] and $Z=2.27a_0$ and $r=2.08a_0$ for Cu(111)[32]]. The larger azimuthal anisotropy for Cu(100) requires that in order to react incident molecules must be oriented not only in the polar direction, but also azimuthally (in the favorable bridge-to-hollow configuration). This will serve to make helicopter reaction somewhat less favored, which explains the lower alignment found in calculations for Cu(100).

Hou *et al.*[1] did not perform velocity-resolved measurements on the alignment of D_2 desorbing from Cu(111) in the $(\nu=0,\ j=4)$ state, so we cannot make a more detailed comparison to their results. However, $A_4^{(2)}$ was obtained in experiments on D_2+Cu(111) in which essentially an average was taken over the desorption energies.[10,11] In both cases, to within the uncertainty of the experimental results, the value found for $A_4^{(2)}$ was zero. From the results of Fig. 3, averaging over the resulting desorption distributions [Eq. (13)], we obtain a value of 0.25 for $A_4^{(2)}$. This is clearly too large compared to the experimental results for D_2+Cu(111). However, the computed number may come down when the calculations are repeated using a PES which has the proper azimuthal anisotropy over the top and hollow sites, and over the intermediate asymmetric sites. It is likely that averaging the alignment curves computed for $(\nu=0,j)$ states with low j for H_2+Cu(111) (Fig. 4 of Ref. 5) over the desorption energy distributions will result in energy-averaged alignments which are too high by even greater amounts, which is a point that was not addressed by Dai and Light in their paper.[5] As already noted, their energy-resolved results were in good agreement with experiment for the two high j-states ($\nu=0$, $j=11$) and ($\nu=1$, $j=6$), for which experiments are available,[1] when the theoretical and experimental results were taken as functions of $E-E_0$.

We now return to Fig. 3. As can be seen from the two upper panels, at low energies (somewhat higher than 0.5 eV), the reaction of ($\nu=0$, $j=4$, $m_j=0$) H_2 is preferred over that of ($\nu=0$, $j=4$, $m_j=1$) H_2, and likewise $R(\nu=0,j=4,m_j=2)>R(\nu=0,j=4,m_j=3)$. A close look at the plots of the reaction probabilities at lower E (not shown here) also reveals higher thresholds (onset energies) for the states with odd m_j than for even-m_j states. These effects are due to the twofold symmetry of the minimum energy barrier (i.e., bridge-to-hollow) in our PES,[34] which is only capable of inducing even transitions in m_j. This means that states with m_j+j odd can only couple to product states in which the H-atom-surface antisymmetric stretch is excited with an odd number of quanta.[22,24,31] Because the product ground state cannot be populated, the threshold is higher and the reaction probability reduced at low E for m_j odd in the present $j=4$ (even) case.

In principle, the symmetry effect seen here could result in an even–odd variation of measured alignment with j at low energies, the alignment for odd j being relatively larger because desorption with $m_j=0$ would be forbidden. Such an effect could be observable for systems having a lowest barrier of C_{2v} symmetry, like H_2+Cu(111), where the effect could serve as a spectroscopic signature of the symmetry of the transition state. However, we anticipate that a high sensitivity would be required to measure this effect. Finally we note that, as discussed in Sec. II A and III A, DFT calculations suggest the existence of a region—which includes the symmetric bridge site and asymmetric sites displaced from it—where the barrier to dissociation is everywhere low. At present it is not clear whether the effects discussed here will show up in calculations if the PES is revised to incorporate the correct azimuthal anisotropy of sites within this transition region.

The reaction probabilities for low-m_j states in Fig. 3 show clear signs of resonances. This aspect has been discussed at some length previously.[4] Similar effects were observed in 2D and 4D calculations (not treating rotation), and were shown to result from a weakening of the H–H bond as the molecule approaches the top site.[21] Although no reso-

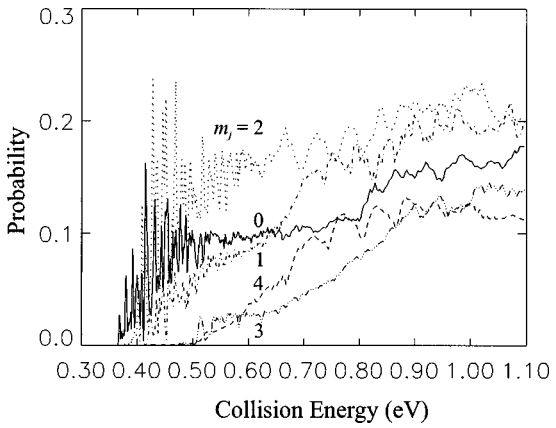

FIG. 5. Vibrational excitation probabilities $P(\nu=0,j=4,m_j \rightarrow \nu'=1)$ are shown for $m_j=0$ (—), $m_j=1$ (·−), $m_j=2$ (···), $m_j=3$ (···−), and $m_j=4$ (−−).

nance calculation has yet been performed for the full 6D system, it is thought a similar mechanism is involved.[4] The fact that the effect is most pronounced for cartwheeling molecules suggests that the resonant states also include some librational motion; initial states with m_j low would then be more likely to populate these librations near the barrier, because they correlate with librationally excited molecule–surface vibrational states.[4]

We next turn our attention to vibrational–excitation probabilities, which are plotted in Fig. 5. Note that the m_j dependence of the vibrational–excitation probability is different from that of the reaction probability (Fig. 3). In particular, vibrational excitation from the ($\nu=0$, $j=4,m_j$) states with $m_j=0-2$ is preferred over vibrational excitation from the states with $m_j=3$ and 4. The dependence of the vibrational–excitation probability on m_j does, nevertheless, correlate in one aspect with the dependence of $R(\nu=0,j=4,m_j)$ on m_j: At high E the $R(\nu=0,j=4,m_j)$ increase with m_j, with reaction of the $m_j=3$ and 4 states being particularly favored. Vibrational excitation, on the other hand, is surprisingly low for these two states, which could point to competition between reaction and vibrational excitation.

To establish the origin of the m_j-dependence of $P(\nu=0,j=4,m_j \rightarrow \nu'=1)$, we have also included in Fig. 6 plots for the final-j-resolved probabilities $P(\nu=0,j=4,m_j \rightarrow \nu'=1,j')$ with $m_j=0$, 2, and 4. This figure shows that the transitions ($\nu=0$, $j=4$, $m_j \rightarrow \nu'=1$, $j'=0$) and ($\nu=0$, $j=4$, $m_j \rightarrow \nu'=1$, $j'=2$) make considerable contributions to the vibrational–excitation probability for $m_j=0$ and 2, but play a diminished role in vibrational–excitation for $m_j=4$ (relative to other contributions). Similarly, the transition ($\nu=0$, $j=4$, $m_j \rightarrow \nu'=1$, $j'=2$) contributes importantly to $P(\nu=0,j=4' \rightarrow \nu'=1)$ for $m_j=1$, but not for $m_j=3$ (results not shown here).

The lower values of $P(\nu=0,j=4,m_j \rightarrow \nu'=1)$ seen for $m_j=3$ and 4 thus appear to result from suppression of downward rotational transitions. This could occur if m_j were to be conserved during vibrational excitation for high-m_j initial states. Indeed, Fig. 7 shows that the $P(\nu=0,j=4,m_j=4 \rightarrow \nu'=1,j'=4,m_j')$ are much larger for $m_j'=m_j$ than for any other values of m_j', suggesting this to be the case. Approximate m_j conservation in vibrational excitation would be expected on physical grounds if the vibrational excitation took place predominantly at sites at which the PES is azimuthally flat. This is the case: vibrational excitation takes place mostly at the top sites[21,63] (a lesser degree of vibrational

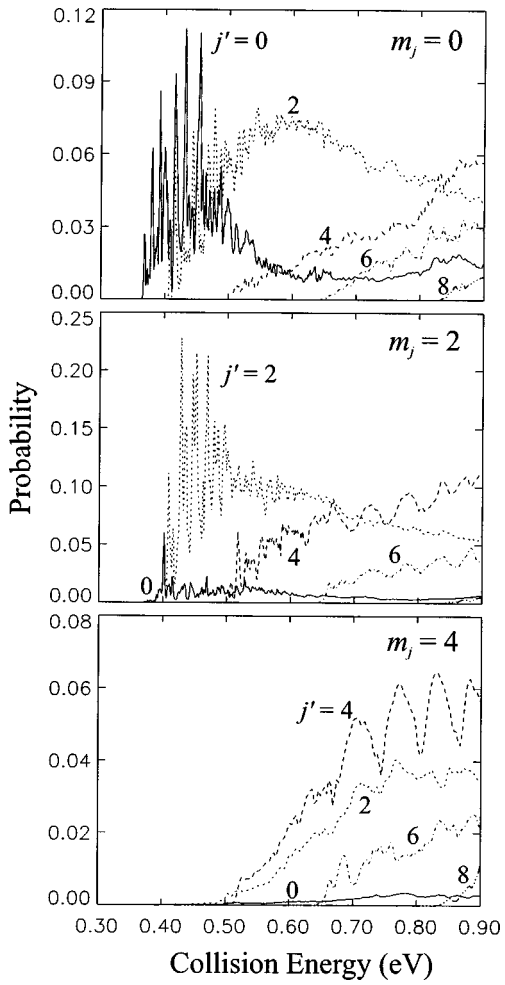

FIG. 6. Vibrational excitation probabilities $P(\nu=0,j=4,m_j \rightarrow \nu'=1,j')$ are shown for three initial states with $m_j=0$, 2, and 4, and for $j'=0$ (—), 2 (···), 4 (−−), 6 (·−), and 8 (···−).

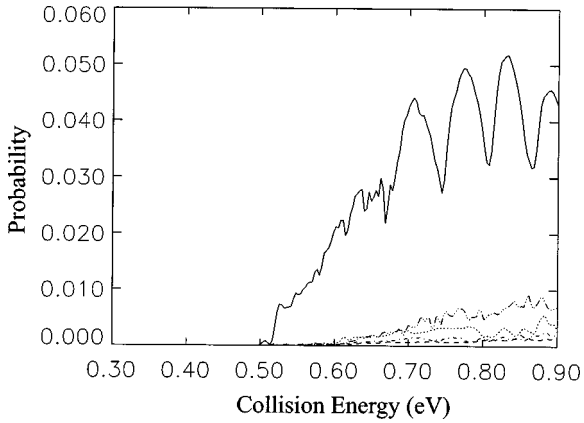

FIG. 7. Vibrational excitation probabilities $P(\nu=0,j=4,m_j=4 \rightarrow \nu'=1,j'=4,m_j')$ are shown for $m_j'=4$ (—), 2 (···), 0 (−−), −2 (·−), and −4 (···−).

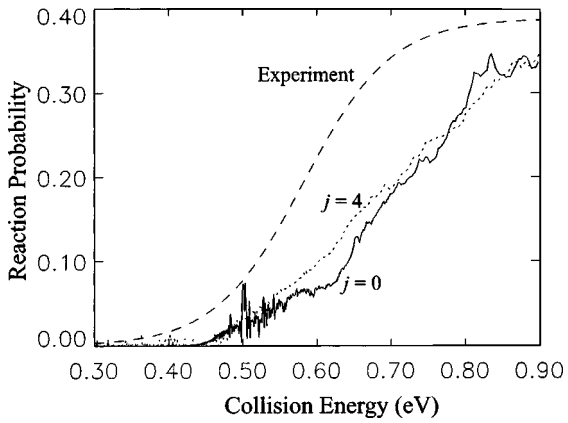

FIG. 8. Collision energy dependence of reaction probabilities for ($\nu=0$, $j=0$) and ($\nu=0$, $j=4$) (averaged over m_j). Also shown is the $\nu=0$ reaction probability calculated from experimental results in Ref. 14.

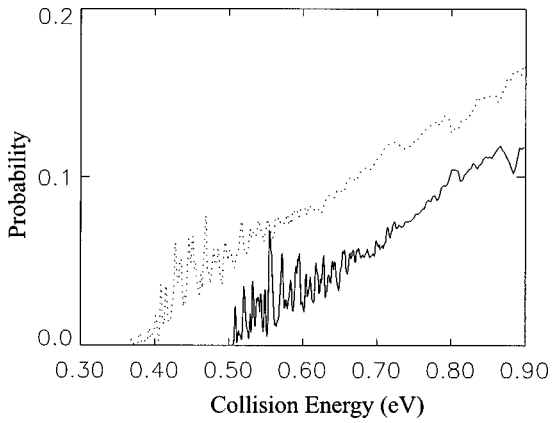

FIG. 9. The vibrational excitation probabilities $P(\nu=0,j=4\rightarrow\nu'=1)$ (···) and $P(\nu=0,j=0\rightarrow\nu'=1)$ (—) are shown.

excitation is seen for collisions with the bridge sites[22,24]). In our PES, the top site has no azimuthal anisotropy associated with it, which explains the observed m_j conservation. Note that, for this site, the lack of azimuthal anisotropy is not necessarily suspect on physical grounds, since the exothermicity associated with the dissociation of the atoms towards the bridge and hollow sites is similar.

As noted before, vibrational excitation also occurs in collisions with the bridge sites. Interestingly, as yet unpublished fixed-site calculations performed for the 4D bridge model show a dependence of $P(\nu=0,j=4,m_j\rightarrow\nu'=1)$ on m_j that is similar to that seen here in the 6D model (reaction of states with $m_j=0$, 1, and 2 is preferred; the 4D results are not shown here). This finding could be related to the observation that in the 4D bridge-site model vibrational excitation takes place for angles in which the molecule is tilted away from orientations with $\theta=90°$. Such orientations are sampled more by the states with low m_j.

We next consider the collision energy dependence of the m_j-averaged reaction probabilities for ($\nu=0$, $j=0$) and ($\nu=0$, $j=4$) (Fig. 8). Associative desorption experiments are currently capable of yielding the energy dependence of *relative j*-resolved probabilities,[12,29] which could be compared with the results presented here. Typically, the experimental results are fitted to a relationship of the type

$$P_{\nu j}(E)=\frac{A_{\nu j}}{2}\left(1+\tanh\frac{E-E_0(\nu,j)}{W_{\nu j}}\right). \tag{16}$$

As already discussed in Ref. 4, the new ($\nu=0$, $j=0$) results show better agreement with a fit[15] to molecular beam[14] and associative desorption[13] experiments than was previously the case.[2,3] As discussed in Sec. II A 1., the first version of the PES[34] contained an artificial well in the entrance channel which steered the molecule towards unfavorable dissociation geometries, thereby diminishing the reaction probability. Because the well has been removed in the current PES, the E_0 (0.69 eV) and A (0.34) values derived from the present $j=0$ results are in better agreement with the fit to experiments ($E_0=0.582$ eV and $A=0.388$) than the previously derived values ($E_0=0.76$ eV and $A=0.28$).

The m_j-averaged reaction probability $R(\nu=0,j=4)$ does not differ much from $R(\nu=0,j=0)$, and $E_0(\nu=0,j=4)\approx E_0(\nu=0,j=0)$. For $E<0.8$ eV, $R(\nu=0,j=4)$ is somewhat larger than $R(\nu=0,j=0)$, suggesting that, at fairly low j, additional rotational excitation helps the reaction. This result is at odds with experiments on associative desorption of H_2 from Cu(111),[12] which found that additional initial rotational energy hinders reaction at low j, while promoting reaction at high j. In particular, reaction of $j=4$ H_2 was suppressed compared with reaction of $j=0$ H_2. The explanation for the hindering is that imparting rotation causes molecules to turn out of reactively favorable orientations before they can reach the barrier, thereby sampling configurations of higher potential and inhibiting reaction (the ability of the molecule to ''steer'' into a favorable orientation is also suppressed by increasing rotation). Imparting even more rotation on the molecule helps dissociation due to increased kinetic coupling between the rotational and dissociative modes (the rotational energy decreases as the bond length increases near the barrier, and the ''lost'' energy is shifted into motion of the H–H bond, which aids reaction). It is possible that the enhanced reaction we find for $j=4$ H_2 relative to $j=0$ H_2 is due to an imbalance between these effects arising from a limitation of the present PES, i.e., the absence of azimuthal anisotropy for the top and hollow sites. In fixed-site studies on the dissociation of H_2 on Cu(111),[16] it was found that azimuthal anisotropy needs to be included in the model to retrieve the correct j-dependence of $E_0(\nu,j)$. In particular, $E_0(\nu,j)$ decreased with increasing j at low j if no azimuthal anisotropy was included in the model. This finding was confirmed in 3D and 4D fixed site calculations on H_2+Cu(100).[24] This suggests that for a correct calculation of the j-dependence of reaction of H_2 on Cu(100), it may be necessary to incorporate the azimuthal anisotropy that is associated with the top and hollow sites in the PES.

In Fig. 9, the vibrational–excitation probabilities $P(\nu=0,j=4\rightarrow\nu'=1)$ and $P(\nu=0,j=0\rightarrow\nu'=1)$ are compared. As can be seen, putting additional rotational energy in the molecule leads to a substantial enhancement of the vibrational excitation probability. This could be expected, because the same kinetic coupling which causes rotational enhancement of reaction could also result in vibrational excitation of

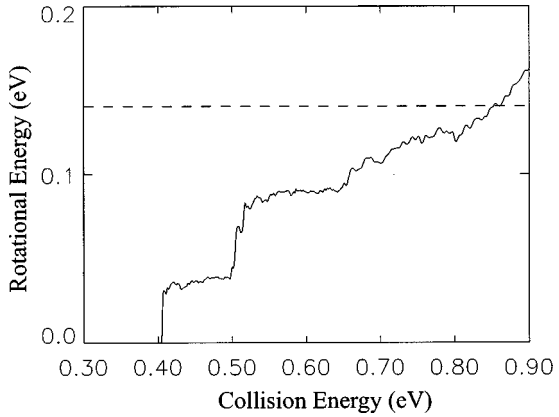

FIG. 10. The average rotational energy is shown as a function of the collision energy, for molecules which are scattered back in $\nu=1$, the scattering taking place from the initial ($\nu=0$, $j=4$) state (with averaging over the initial m_j). The dashed line indicates the initial rotational energy of H_2.

the reflected portion of the wavepacket. At $E=0.9$ eV, $P(\nu=0,j=4\rightarrow\nu'=1)=0.17$, in rough agreement with the vibrational excitation probability $P(\nu=0\rightarrow\nu'=1,j'=3)$ (0.28) that was found for high E in experiments on H_2+Cu(111) by Rettner *et al.*[33]

Our results may be of some help with the interpretation of these experiments. The molecular beam experiments measure the time-of-flight (TOF) distributions that are associated with excited rovibrational ($\nu=1,j$) states, both in the incoming and scattered beam. Typically, a peak is observed in the TOF spectrum at high E (short times), which is attributed to vibrational excitation of molecules in ($\nu=0,j,m_j$) states that are also in the beam. From which ($\nu=0,j,m_i$) states the excitation to the ($\nu=1,j$) proceeds could not be established in the experiments. However, the observation that the measured maximum value of $P(\nu=0\rightarrow\nu'=1,j')$ decreased with increasing j'[64] led to speculation that vibrational excitation could be accompanied (and promoted) by simultaneously occurring rotational de-excitation. As Fig. 6 shows, the transitions ($\nu=0$, $j=4$, $m_j\rightarrow\nu'=1,j'$) with $j'=0$ and 2 indeed make important contributions to $P(\nu=0,j=4\rightarrow\nu'=1)$. Furthermore, as Fig. 10 shows, vibrational excitation is accompanied by rotational energy loss for all but the highest E. When plotted as a function of the total (collision+internal) energy, the $P(\nu=0,j=4\rightarrow\nu'=1)$ and $P(\nu=0,j=0\rightarrow\nu'=1)$ shown in Fig. 9 are nearly superimposed, suggesting very efficient conversion of initial rotational energy to vibrational energy. Finally, the experimentalists have speculated that the m_j dependence of the vibrational excitation probability $P(\nu=0,j,m_j\rightarrow\nu'=1)$ should not be as simple as that of the reaction probability;[33] inspection of Fig. 5 and Fig. 3 confirm this suggestion for the example of ($\nu=0$, $j=4$) scattering from Cu(100) that is studied here.

IV. CONCLUSIONS

We have used the symmetry-adapted wave-packet method to perform calculations for H_2 dissociatively adsorbing on Cu(100). The PES used is an improved fit to points calculated using density-functional theory (DFT), with the generalized gradient approximation (GGA), and a slab representation for the surface. The method, which was developed in earlier work,[2–4] has here been extended so as to treat initial states with m_j odd. In such cases, the initial nonsymmetry-adapted state can be decomposed into two symmetry-adapted states which are partners in an irreducible representation of species E. We have demonstrated that unlike calculations for states with even and nonzero m_j, where wavepackets must be propagated for two separate symmetries,[4] when m_j is odd only one of the two partner wave-packets needs propagating: Results for both partners can be derived from this single calculation. No additional computational saving results, however, because the basis size for each E partner species is approximately double that of other species (e.g., A_2, B_1, etc.). (Note that there is still a dramatic computational saving over the standard nonsymmetry-adapted wave-packet method.)

Reaction probabilities for all ($\nu=0$, $j=4$, m_j) initial states have been presented. The reaction of the helicopter ($|m_j|=j$) state is preferred over that of the cartwheel state for $E>0.44$ eV. At high E, for one and the same energy, the reaction probability simply increases with m_j. At lower E, in contravention of this trend, we find that $R(\nu=0,j=4,m_j=0)>R(\nu=0,j=4,m_j=1)$, and that $R(\nu=0,j=4,m_j=2)>R(\nu=0,j=4,m_j=3)$. The latter finding is a consequence of the $\Delta m_j=$even selection rule that follows from the way the PES is constructed, the selection rule being that states with $j+m_j$ odd should react less well at low energies because they connect only to H-atom–surface vibrational states in which the antisymmetric stretch vibration is excited. However, we suggest that the finding may be general for systems in which the lowest barrier to dissociation occurs at a site of $C_{2\nu}$ symmetry. This could lead to odd–even alternations of the quadrupole alignment with j that would be observed for (ν,j) H_2 desorbing from the surface, which would serve as a spectroscopic signature of the transition state.

The energy dependence of the quadrupole alignment obtained from the $R(\nu=0,j=4,m_j)$ curves using detailed balance is in qualitative agreement with that observed in velocity-resolved experiments on ($\nu=0$, $j=11$) and ($\nu=1$, $j=6$) D_2 desorbing from Cu(111). That is, the alignment is a positive, decreasing function of E for desorption energies larger than $E_0-0.2$ eV, which is the range of energies for which experiments were performed [E_0 is the dynamical barrier height, i.e., the value of the collision energy at which the reaction probability of ($\nu=0$, $j=4$) H_2 is at half its maximum value ($\approx$0.69 eV)]. In contrast, the value that is obtained for the alignment (0.25) when averaging over the desorption energy distribution is too large compared to experiments for ($\nu=0$, $j=4$) D_2+Cu(111), in which energy-averaged values of essentially zero were obtained.

The reaction probability $R(\nu=0,j=0)$ that is obtained for the improved PES is in better agreement with experimental results than previous calculations, the theoretical value of the dynamical barrier height now being too high by only 0.11 eV (previously 0.18 eV). Our finding that $R(\nu=0,j=4)$ (obtained by averaging over m_j) exceeds $R(\nu=0,j=0)$ for most collision energies is at odds with experiments for H_2+Cu(111) in which it was found that additional rotation

hinders reaction for low j. The discrepancy is possibly due to a defect in our present PES, which assumes that there is no azimuthal anisotropy associated with the high symmetry top and hollow sites. Also, the present PES does not yet correctly describe a particular asymmetric transition state, for which electronic structure calculations presented here show that the azimuthal anisotropy is even larger than that associated with the bridge site. The electronic structure calculations also confirm previous findings that the lowest energy barrier at the asymmetric site is even lower than the lowest barrier found for the bridge site (by $\approx$30 meV), which serves to further underline the desirability of extending the present PES. Due to its having too little azimuthal anisotropy at the top, hollow, and asymmetric site discussed above, calculations performed with this PES should overestimate the alignment at low and high energies.

In agreement with molecular beam experiments performed for H_2 and D_2+Cu(111), our calculations show substantial vibrational excitation of H_2 colliding with Cu(100). The vibrational excitation probability for the $(\nu=0,\ j=4)$ state is much larger than for the $(\nu=0,\ j=0)$ initial state. Vibrational excitation is accompanied by loss of rotational energy for all but the highest collision energies, as was also suggested by the experiments. The dependence of the vibrational–excitation probability on m_j is not as simple as that of the initial-state-resolved reaction probability, $P(\nu=0,j=4,m_j\rightarrow\nu'=1)$ being larger for $m_j=0-2$ than for $m_j=3$ and 4.

ACKNOWLEDGMENTS

We wish to thank H. Hou for answering questions pertaining to the experimental accuracy of associative desorption measurements, and D. A. Auerbach and A. M. Wodtke for helpful discussions. We also thank B. Hammer and P. Kratzer for communicating their electronic structure results, and J. Dai for supplying an electronic copy of his H_2+Cu(111) LEPS potential. Thanks are also due to G. Wiesenekker, who computed the PES for H_2+Cu(100), and J. G. Snijders, for his help with symmetry aspects. This research was made possible by the National Computing Facilities Foundation (NCF) and Cray Research Inc., through an NCF/Cray Research University Grant and allocation of computer time. We also acknowledge the support of the Royal Netherlands Academy of Arts and Sciences (KNAW). Work at NRL was funded by the Office of Naval Research through the NRL. This work was supported in part by a grant of HPC time from the DoD HPC Center, Army Research Laboratory Cray T-90.

[1] H. Hou, S. J. Gulding, C. T. Rettner, A. M. Wodtke, and D. J. Auerbach, Science **277**, 80 (1997).
[2] G. J. Kroes, E. J. Baerends, and R. C. Mowrey, Phys. Rev. Lett. **78**, 3583 (1997).
[3] G. J. Kroes, E. J. Baerends, and R. C. Mowrey, J. Chem. Phys. **107**, 3309 (1997).
[4] D. A. McCormack, G. J. Kroes, E. J. Baerends, and R. C. Mowrey, Faraday Discuss **110**, 267 (1998).
[5] J. Dai and J. C. Light, J. Chem. Phys. **108**, 7816 (1998).
[6] J. Dai and J. C. Light, J. Chem. Phys. **107**, 1676 (1997).
[7] A. Gross, B. Hammer, M. Scheffler, and W. Brenig, Phys. Rev. Lett. **73**, 3121 (1994).
[8] A. Gross, S. Wilke, and M. Scheffler, Phys. Rev. Lett. **75**, 2718 (1995).
[9] D. Wetzig, R. Dopheide, M. Rutkowski, R. David, and H. Zacharias, Phys. Rev. Lett. **76**, 463 (1996).
[10] D. Wetzig, M. Rutkowski, R. David, and H. Zacharias, Europhys. Lett. **36**, 31 (1996).
[11] S. J. Gulding, A. M. Wodtke, H. Hou, C. T. Rettner, H. A. Michelsen, and D. J. Auerbach, J. Chem. Phys. **105**, 9702 (1996).
[12] C. T. Rettner, H. A. Michelsen, and D. J. Auerbach, J. Chem. Phys. **102**, 4625 (1995).
[13] G. Comsa and R. David, Surf. Sci. **117**, 77 (1982).
[14] G. Anger, A. Winkler, and K. D. Rendulic, Surf. Sci. **220**, 1 (1989).
[15] H. A. Michelsen and D. J. Auerbach, J. Chem. Phys. **94**, 7502 (1991).
[16] G. R. Darling and S. Holloway, J. Chem. Phys. **101**, 3268 (1994).
[17] C. Engdahl, B. I. Lundqvist, U. Nielsen, and J. K. Nørskov, Phys. Rev. B **45**, 11362 (1992).
[18] U. Nielsen, D. Halstead, S. Holloway, and J. K. Nøskov, J. Chem. Phys. **93**, 2879 (1990).
[19] M. Hand and S. Holloway, Surf. Sci. **211/212**, 940 (1989).
[20] M. R. Hand and S. Holloway, J. Chem. Phys. **91**, 7209 (1989).
[21] G. J. Kroes, G. Wiesenekker, E. J. Baerends, R. C. Mowrey, and D. Neuhauser, J. Chem. Phys. **105**, 5979 (1995).
[22] R. C. Mowrey, G. J. Kroes, G. Wiesenekker, and E. J. Baerends, J. Chem. Phys. **106**, 4248 (1997).
[23] J. Dai and J. Z. H. Zhang, J. Chem. Phys. **102**, 6280 (1995).
[24] R. C. Mowrey, G. J. Kroes, and E. J. Baerends, J. Chem. Phys. **108**, 6906 (1998).
[25] J. Dai, J. Sheng, and J. Z. H. Zhang, J. Chem. Phys. **101**, 1555 (1994).
[26] J. Dai and J. Z. H. Zhang, Surf. Sci. **319**, 193 (1994).
[27] T. Brunner and W. Brenig, Surf. Sci. **317**, 303 (1994).
[28] G. R. Darling and S. Holloway, Faraday Discuss. Chem. Soc. **96**, 43 (1993).
[29] H. A. Michelsen, C. T. Rettner, D. J. Auerbach, and R. N. Zare, J. Chem. Phys. **98**, 8294 (1993).
[30] J. Sheng and J. Z. H. Zhang, J. Chem. Phys. **99**, 1373 (1993).
[31] J. Sheng and J. Z. H. Zhang, J. Chem. Phys. **97**, 6784 (1992).
[32] B. Hammer, M. Scheffler, K. W. Jacobsen, and J. K. Nørskov, Phys. Rev. Lett. **73**, 1400 (1994).
[33] C. T. Rettner, H. A. Michelsen, and D. J. Auerbach, Chem. Phys. **175**, 157 (1993).
[34] G. Wiesenekker, G. J. Kroes, and E. J. Baerends, J. Chem. Phys. **104**, 7344 (1996).
[35] P. Kratzer, B. Hammer, and J. K. Nørskov, Surf. Sci. **359**, 45 (1996).
[36] J. A. White, D. M. Bird, M. C. Payne, and I. Stich, Phys. Rev. Lett. **73**, 1404 (1994).
[37] G. te Velde and E. J. Baerends, Phys. Rev. B **44**, 7888 (1991).
[38] G. te Velde and E. J. Baerends, J. Comput. Phys. **99**, 84 (1992).
[39] P. Hohenberg and W. Kohn, Phys. Rev. **136**, B864 (1964).
[40] W. Kohn and L. J. Sham, Phys. Rev. **140**, A1133 (1965).
[41] F. Herman and S. Skillman, *Atomic Structure Calculations* (Prentice-Hall, New Jersey, 1963).
[42] G. Wiesenekker, G. te Velde, and E. J. Baerends, J. Phys. C **21**, 4263 (1988).
[43] S. H. Vosko, L. Wilk, and M. Nusair, Can. J. Phys. **58**, 1200 (1980).
[44] A. D. Becke, Phys. Rev. A **38**, 3098 (1988).
[45] J. P. Perdew, Phys. Rev. B **33**, 8822 (1986).
[46] J. P. Perdew, in *Electronic structure of Solids '91*, edited by P. Ziesche and H. Eschnig (Akademie Verlag, Berlin, 1991).
[47] J. P. Perdew, J. A. Chevary, S. H. Vosko, K. A. Jackson, M. R. Pederson, D. J. Singh, and C. Fiolhais, Phys. Rev. B **46**, 6671 (1992).
[48] G. te Velde, Ph.D. thesis, Vrije Universiteit, Amsterdam (1990).
[49] A. Messiah, *Quantum Mechanics Vol. 1* (North Holland, Amsterdam, 1961).
[50] G. J. Kroes, J. G. Snijders, and R. C. Mowrey, J. Chem. Phys. **102**, 5512 (1995).
[51] G. J. Kroes, J. G. Snijders, and R. C. Mowrey, J. Chem. Phys. **103**, 5121 (1995).
[52] G. Burns, *Introduction to Group Theory with Applications* (Academic, New York, 1977).
[53] P. W. Atkins, *Molecular Quantum Mechanics*, 2nd ed. (Oxford University Press, Oxford, 1983).

[54] J. A. Salthouse and M. J. Ware, *Point Group Character Tables and Related Data* (North-Holland, Amsterdam, 1967).
[55] R. McWeeny, *The International Encyclopedia of Physical Chemistry and Chemical Physics, Topic 1. Mathematical Techniques, Vol. 3 Symmetry* (Pergamon, Oxford, 1963).
[56] V. A. Mandelshtam and H. S. Taylor, J. Chem. Phys. **103**, 2903 (1995).
[57] G. G. Balint-Kurti, R. N. Dixon, and C. C. Marston, J. Chem. Soc., Faraday Trans. **86**, 1741 (1990); Int. Rev. Phys. Chem. **11**, 317 (1992).
[58] R. C. Mowrey and G. J. Kroes, J. Chem. Phys. **103**, 1216 (1995).
[59] G. Wiesenekker, G. J. Kroes, E. J. Baerends, and R. C. Mowrey, J. Chem. Phys. **102**, 3873 (1995); **103**, 5168 (1995).
[60] P. Kratzer (private communication).
[61] H. Hou (private communication).
[62] R. N. Zare, *Angular Momentum* (Wiley, New York, 1988).
[63] G. J. Kroes, G. Wiesenekker, E. J. Baerends, and R. C. Mowrey, Phys. Rev. B **53**, 10397 (1996).
[64] C. T. Rettner, D. J. Auerbach, and H. A. Michelsen, Phys. Rev. Lett. **68**, 2547 (1992).